A C-band hat-fed reflector antenna

Su Yee Aye (1), Tse Tong Chia (2), Sigurd Huber (3), and Koen Mouthaan (1)
(1) Electrical and Computering Engineering, National University of Singapore, Singapore
(2) Temasek Laboratories, National University of Singapore, Singapore
(3) Microwaves and Radar Institute, German Aerospace Center (DLR), Oberpfaffenhofen, Germany

The hat-fed reflector antenna is a compact type of center-fed reflector antenna where the feed is located along the axis of the reflector without supporting struts. The ratios of focal length *F* and the diameter *D* of the compact reflector antennas are small and in the range of 0.2-0.4. The sub-reflector is usually supported by a dielectric, which is located on top of the waveguide. The advantages of the compact reflector antennas are (1) its low profile, (2) no struts required to support the feed and the sub-reflector, and consequently (3) improvements in antenna performance particularly in sidelobe levels and gain that are normally degraded by the presence of the struts. However, the disadvantage of the compact design is that the feed protruding in the middle of the reflector can raise coupling interactions with the reflector. To consider the complicated field interactions among the feed, dielectric parts, sub-reflector and main reflector, a full-wave electromagnetic analysis of the entire antenna is necessary. The self-fed reflector antennas have been investigated mainly for satellite communication, using circular polarization. When considering surveillance detection applications, these antennas are promising because of their compact and light-weight structures with high gain capability. This research work presents the design of a C-band (5.2-6.2 GHz) dual-linear polarized feed for a parabolic reflector with an F/D ratio of 0.37. The reflector diameter *D* is 0.9 meter ($17\lambda_c$), and the focal length *F* is 0.33 meter ($6\lambda_c$), in which λ_c represents the wavelength of the center frequency. Fig. 1(a) depicts the feed which consists of a circular waveguide, a dielectric taper, a dielectric neck and a sub-reflector hat.

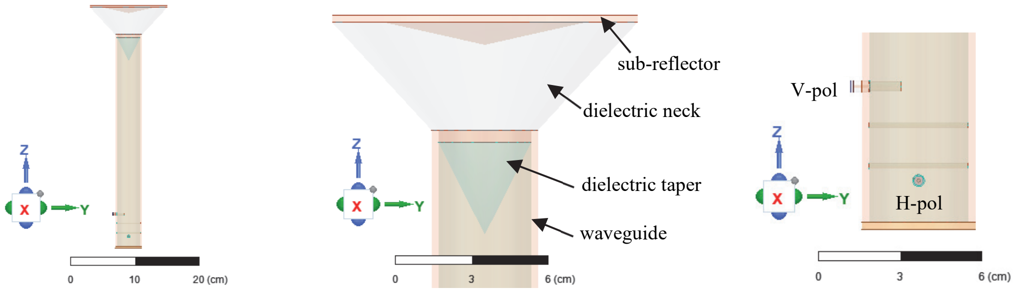

(a) (b) (c)

Fig. 1. (a) Optimized feed. (b) Enlarged view. (c) Dual-pol coaxial-to-waveguide transition.

The inner diameter of the waveguide is 3.7 cm. The dielectric material is polycarbonate ($\varepsilon_r = 2.9$ and $\tan \delta = 0.01$), and the conducting material is aluminium. The feed without the reflector is optimized in HFSS with the goals: (i) return loss to be larger than 15 dB over the considered frequency band, (ii) 10 dB edge taper at the reflector subtended angle, (iii) minimum possible reflections from the sub-reflector back into the waveguide, and (iv) the feed patterns in the E-plane and H-plane to be similar to each other. In fact, Fig. 1(a) represents the optimized feed, which has been fabricated in the workshop for the next stage of test and measurement with the reflector. Fig. 1(b) shows the zoomed view of the sub-reflector and associated dielectric parts. Fig.1 (c) illustrates the coaxial-to-waveguide transition for the dual-pol excitation. The excitation ports have 50 Ω impedance. Fig. 2 (a) represents the simulation set-up of the reflector antenna in HFSS. Finite Element Boundary Integral (FE-BI) radiation boundary is applied to the air region enclosing the feed. The feed including the sub-reflector is solved using the Finite Element Method. The main reflector is set to Physical Optics (PO) region. The field interactions between the FE-BI and PO regions are through two-way coupling. The realized gain versus frequency plot of the V-pol and H-pol excitations is shown in Fig. 2 (b). The gains are greater than 30 dB and the gain variations are within 1.9 dB over the 1 GHz bandwidth. The realized gain patterns in the E-plane and H-plane at 5.6 GHz are shown in Fig. 3(a) and Fig. 3(b), respectively. The peak-to-sidelobe ratios are 19.3 dB and 16.1 dB in the E-plane and H-plane. The sidelobes beyond ±30° are around -10 dB in the E-plane. In the H-plane, there is a higher sidelobe around ±90° due to the spill-over radiation of the feed beyond the reflector subtended angle of 68°. The spill-over effect is directly seen as a raised side lobe in the region beyond ±68°. Cross polarization is noticed to be high and around 26 dB in both principal planes. The cross polarization can be improved by optimizing or re-designing the waveguide transition adaptor. The dual-pol adapter was purchased from a company and can be further improved. Another alternative to improve the returned signals from the sub-reflector in the waveguide is to adjust the length of the waveguide.

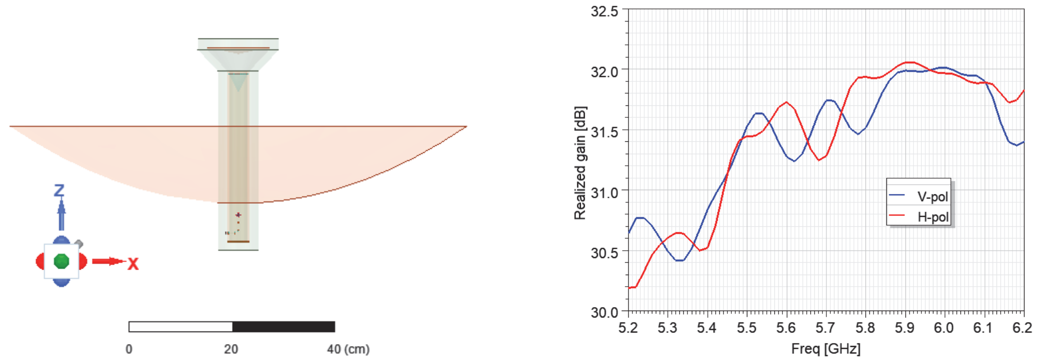

(a) (b)

Fig. 2. (a) Simulation set-up of the reflector antenna in HFSS. (b) Realized gain versus frequency of the reflector antenna for V-pol and H-pol excitations.

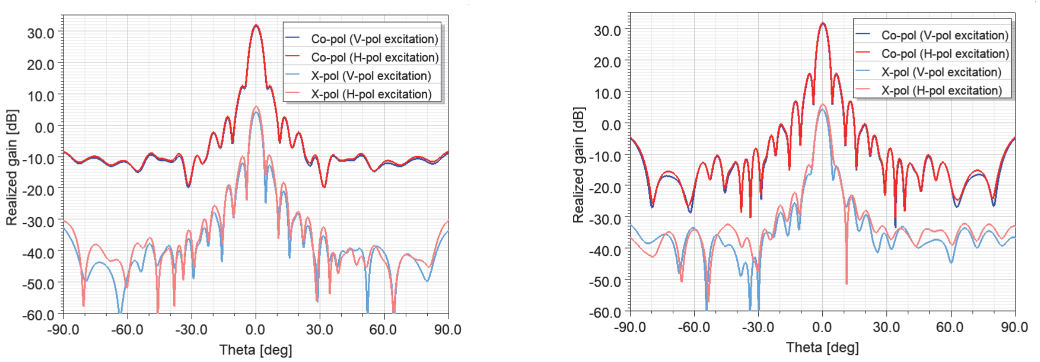

(a) (b)

Fig. 3. Patterns of the reflector antenna at 5.6 GHz. (a) E-plane. (b) H-plane.

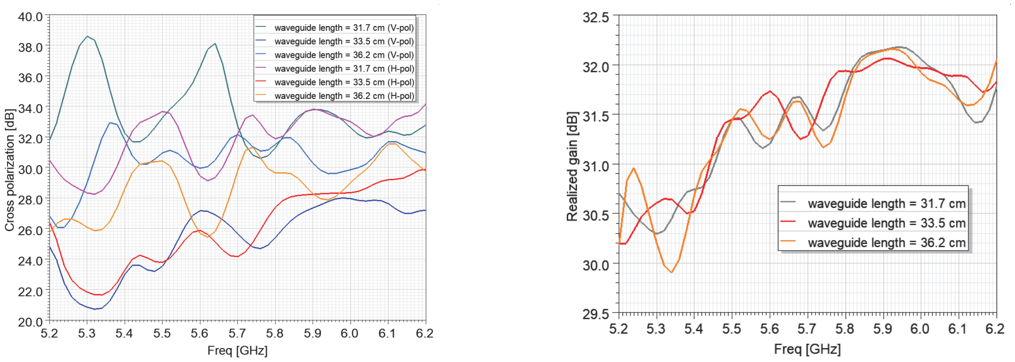

(a) (b)

Fig. 4. (a) Cross polarization versus frequency. (b) Realized gain versus frequency of the reflector antenna with different waveguide lengths.

The gain and cross polarization versus frequency of three different waveguide lengths are compared in Fig. 4. The peaks of the reflector antenna are not much affected by changing the waveguide length. However, it is noted that the cross polarization varies up to 18 dB with the changes in the waveguide length. The waveguide length of 31.7 cm can provide the cross polarization of 32 dB on average.

Radiation patterns of the reflector antenna will be measured in two principal planes of each polarization for the considered frequency range. Measurement results will be presented at the workshop.